

Colorimetric Biosensors Based on DNAzyme-Assembled Gold Nanoparticles

Juewen Liu¹ and Yi Lu^{1,2}

Received December 17, 2003; accepted March 20, 2004

Taking advantage of recent developments in the field of metallic nanoparticle-based colorimetric DNA detection and in the field of *in vitro* selection of functional DNA/RNA that can recognize a wide range of analytes, we have designed highly sensitive and selective colorimetric biosensors for many analytes of choice. As an example of the sensor design strategy, a highly sensitive and selective colorimetric lead biosensor based on DNAzyme-directed assembly of gold nanoparticles is reviewed. The DNAzyme consists of an enzyme and a substrate strand, which can be used to assemble DNA-functionalized gold nanoparticles. The aggregation brings gold nanoparticles together, resulting in a blue-colored nanoparticle assembly. In the presence of lead, the DNAzyme catalyzes specific hydrolytic cleavage of the substrate strand, which disrupts the formation of the nanoparticle assembly, resulting in red-colored individual nanoparticles. The application of the sensor in lead detection in leaded paint is also demonstrated. In perspective, the use of allosteric DNA/RNAzymes to expand the range of the nanoparticle-based sensor design method is described.

KEY WORDS: Nanoparticles; colorimetric; biosensors; aptamers; DNAzymes.

INTRODUCTION

The intense red color of gold nanoparticles has attracted scientific attention for more than four centuries [1,2]. In biology, gold nanoparticles were mainly used as labeling reagents for microscopy [2]. In 1996, Mirkin and co-workers reported the functionalization of gold nanoparticles with thiol-modified DNA [3]. Upon addition of DNA strands that are complementary to the DNA attached to gold nanoparticles, DNA-functionalized nanoparticles can aggregate reversibly due to DNA base-pairing interactions, accompanied by a red-to-blue color transition. The change of color results from the shift of the surface plasmon band of gold nanoparticles upon aggregation, and this property has been subsequently used to design colorimet-

ric biosensors for selective detection of DNA [4–6]. The nanoparticle-based DNA detection has been shown to be not only simple, but also highly sensitive and selective, and can rival other detection methods, such as those based on fluorescence.

Over the years, remarkable progress has been made on the design of nanoparticle-based colorimetric biosensors. For example, besides gold nanoparticles, Ag/Au core-shell nanoparticles [7], and quantum dots [8], such as CdSe/ZnS core-shell nanoparticles have been functionalized with DNA and shown potential application as biosensors. Recently, peptide nucleic acids (PNA) have been used to replace DNA to functionalize gold nanoparticles [9]. Upon hybridization to complementary DNA strands and formation of nanoparticle aggregates, the stability of PNA-functionalized gold nanoparticles increases, allowing even higher discrimination of DNA single-base mismatches.

The sensors for highly sensitive and selective DNA detection mentioned above are based on using the target DNA molecule as a cross-linking reagent. In a recent

¹ Department of Chemistry, University of Illinois at Urbana – Champaign, Urbana, Illinois.

² To whom correspondence should be addressed at Department of Chemistry, University of Illinois – Champaign, Urbana, Illinois 61801. E-mail: yi-lu@uiuc.edu

communication, a non-cross-linking-based approach to gold nanoparticle-based aggregation assays for DNA detection was reported, which is also capable of single-base-mismatch discrimination [10]. The authors proposed that the formation of perfectly matched base pairs to the DNA attached to nanoparticles could reduce the repulsive interactions among nanoparticles. Besides detection methods based on the aggregation of gold nanoparticles, a simple scanometric method has been developed, taking the advantage of gold nanoparticle-catalyzed reduction of silver [6]. With the increasingly important role that the metallic nanoparticle-based detection method is playing in diagnostics and genomic research, it is very desirable to apply this detection method beyond simple DNA detection to the detection of essentially any analyte of interest.

Biology provides the best opportunity to achieve the above goal. The development of a powerful combinatorial biology technique called *in vitro* selection or systematic evolution of ligands by exponential enrichment (SELEX) in the early 1990s [11–15] made it possible to obtain functional DNA/RNA molecules that can bind to a wide range of analytes with high affinity and specificity [16–20]. A list of analytes that can be recognized by these DNA/RNA molecules (called aptamers) is presented in Table I. It can be seen from the table that the range of analytes covers from those as simple as metal ions to as complicated as whole cells and even intact viral particles.

A particularly interesting class of *in vitro* selected DNA/RNA are catalytically active DNA/RNA that can catalyze many of the same reactions as protein enzymes [77–81]. Catalytic RNA molecules have been found in nature and are known as ribozymes [82,83], which will be referred to in this paper as RNAzymes. A list of reactions that RNAzymes can catalyze is presented in Table II. Long considered as strictly a genetic information storage material, DNA was shown in 1994 to carry out catalytic functions and thus became the newest member of the enzyme family after proteins and RNA [99]. Catalytically active DNA molecules are called DNAzymes in this paper and are also known as deoxyribozymes, DNA enzymes or catalytic DNA elsewhere. Although no naturally occurring DNAzymes have been found, DNAzymes that can catalyze a variety of reactions have been isolated through the *in vitro* selection method [78,80,100,101]. In Table III, a list of reactions that DNA can catalyze is presented. Importantly, the activity of DNA/RNAzymes can be tuned in the selection process by varying cofactors and cofactor concentrations, so that the activity of resulting DNA/RNAzymes could be dependent on those cofactors (analytes). Therefore, these analyte-dependent DNA/RNAzymes can be used to design biosensors to detect those analytes.

DNAzymes are especially attractive as a platform to design biosensors. First, many analyte-dependent

Table I. Analytes That Can Be Recognized by DNA/RNA Aptamers

Analyte type	Examples and references
Metal ions	K(I)[21], Zn(II)[22], Ni(II)[23]
Organic dyes	Cibacron blue and Reactive green 19[24,25], Sulforhodamine B[26], Malachite green [27]
Small organic molecules	Biotin[28], Cocaine[29], Theophylline[30], Adenine[31], Dopamine[32]
Amino acids	l-Valine[33], d-Tryptophan[34], Arginine[35–37], Citrulline[38]
Nucleosides/nucleotides	Guanosine[39], ATP[40,41], GTP[42], cAMP[43]
Nucleotide analogs	8-oxo-dG[44], 7-Me-guanosine
RNA	TAR-RNA[45]
Biological cofactors	NAD[46], FMN[46,47], Porphyrins[48], Vitamin B12[49], FAD[50], CoA[51]
Aminoglycosides	Tobramycin[52], Neomycin [53]
Oligosaccharides	Cellulose[54]
Polysaccharides	Sephadex[55]
Antibiotics	Streptomycin[56], Viomycin[57], Tetracycline[58]
Peptides	Rev peptide[59], Vasopressin[60], Substance P[61]
Enzymes	Human Thrombin[62], HIV Rev Transcriptase[63], Fpg[64] Human RNase H1[65]
Growth factors	Keratinocyte GF[66], Basic fibroblast GF[67], VEGF ₁₆₅ [68]
Transcription factors	NF- κ B[69]
Antibodies	Human IgE[70]
Gene regulatory factors	Elongation factor Tu[71]
Cell adhesion molecules	Human CD4[72], Selectin[73]
Cells	YPEN-1 endothelial cells[74]
Intact viral/bacterial particles	Rous sarcoma virus[75], Anthrax spores[76]

Table II. Reactions Catalyzed by RNAzymes That Were Isolated from *In Vitro* Selection Experiments

Reaction	k_{cat}	K_m (μM)	$k_{\text{cat}}/k_{\text{uncat}}^a$	Reference
<i>Phosphoester centers</i>				
Cleavage	0.1	0.03	10^5	[84]
Transfer	0.3	0.02	10^{13}	[77]
Ligation	100	9	10^9	[85]
Phosphorylation	0.3	40	$>10^5$	[86]
Mononucleotide polymerization	0.3	5000	$>10^7$	[87]
<i>Carbon centers</i>				
Aminoacylation	1	9000	10^6	[88]
Aminoacyl ester hydrolysis	0.02	0.5	10	[89]
Aminoacyl transfer	0.2	0.05	10^3	[90]
<i>N</i> -alkylation	0.6	1000	10^7	[91]
<i>S</i> -alkylation	4×10^{-3}	370	10^3	[92]
Amide bond cleavage	1×10^{-5}		10^2	[93]
Amide bond formation	0.04	2	10^5	[94]
Peptide bond formation	0.05	200	10^6	[95]
Diels-Alder cycloaddition	>0.1	>500	10^3	[96]
<i>Others</i>				
Biphenyl isomerization	3×10^{-5}	500	10^2	[97]
Porphyrin metallation	0.9	10	10^3	[98]

Note. Table II and Table III were adapted from "The RNA world," 2nd ed., Cold Spring Harbor Laboratory Press, 1999, pp. 687–689.

^aReactions catalyzed by RNAzymes that were isolated from *in vitro* selection experiments. $k_{\text{cat}}/k_{\text{uncat}}$ is the rate enhancement over uncatalyzed reaction.

DNAzymes have already been isolated (Table III). Second, DNA molecules have higher stability than proteins and RNA and can be denatured and renatured many times without losing their catalytic or binding abilities. Third, DNA is relatively less expensive to produce, and the solid phase DNA synthesis chemistry can produce DNA with various functional groups conveniently. An example of *in vitro* selection of DNAzymes that have analyte-dependent activities is shown in Fig. 1. A small population of DNAzymes with desired properties are selected and amplified from a pool of up to 10^{15} random DNA sequences. The selected DNAzymes are then subjected to further rounds of mutation and amplification and re-selection, often with more

stringent selection conditions. When the activity of the pool stops increasing, the pool is cloned and sequenced to obtain the active DNAzyme sequences.

The development of the nanotechnology of DNA-functionalized gold nanoparticles and the development of the biotechnology of the *in vitro* selection of target specific nucleic acids offer us a unique opportunity to combine these two emerging fields to design colorimetric biosensors that can detect a very wide range of analytes. In this paper, a brief review of the initial efforts made in our group to design colorimetric biosensors is presented. We chose an *in vitro* selected DNAzyme (named the "8-17" DNAzyme [104,107,114]) with high selectivity for Pb^{2+}

Table III. DNAzymes Isolated Through *In Vitro* Selection

Reaction	Cofactor	k_{max} (min^{-1}) ^a	$k_{\text{cat}}/k_{\text{uncat}}$	Reference
RNA transesterification	Pb^{2+}	1	10^5	[99]
	Mg^{2+}	0.01	10^5	[102]
	Ca^{2+}	0.08	10^5	[103]
	Mg^{2+}	10	$>10^5$	[104]
	None	0.01	10^8	[105]
	L-Histidine	0.2	10^6	[106]
	Zn^{2+}	~ 40	$>10^5$	[107]
DNA cleavage	Cu^{2+}	0.2	$>10^6$	[108]
DNA ligation	Cu^{2+} or Zn^{2+}	0.07	10^5	[109]
RNA ligation	Mn^{2+}	2.2	$>10^6$	[110]
DNA phosphorylation	Ca^{2+}	0.01	10^9	[111]
5',5'-pyrophosphate formation	Cu^{2+}	5×10^{-1}	$>10^{10}$	[112]
Porphyrin metallation	None	1.3	10^3	[113]

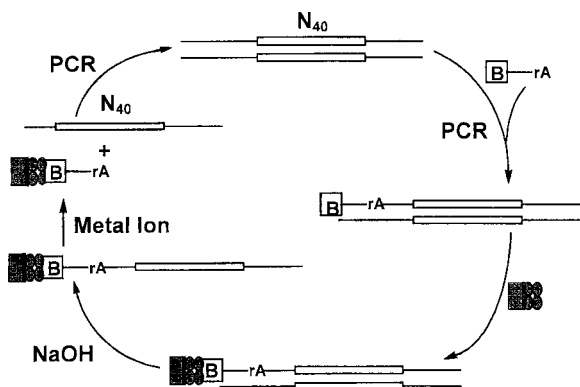


Fig. 1. An example of *in vitro* selection of DNAzymes with RNA endonuclease activity. The initial selection pool (top left) contains a random sequence domain of 40 nucleotides (shown as a bar) flanked by two conserved primer-binding regions (shown as single lines). After one polymerase chain reaction (PCR) reaction to amplify the DNA pool, a second PCR reaction is performed in which one of the PCR primers contains a biotin moiety (**B**) at the 5'-end, and a ribonucleic adenosine (**rA**) embedded in the 5'-conserved sequence region. The **rA** is intended to be the cleavage site due to the relative lability of the RNA bond toward hydrolytic cleavage. The DNA pool is then immobilized on an avidin column through the biotin moiety on the 5'-end of the DNA. Since single stranded DNA molecules are most likely to form complex three-dimensional structure necessary for DNAzyme function, the double stranded DNA molecules are denatured by NaOH and the DNA strand without biotin can be washed away from the column. Addition of metal ions to the column containing the remaining single-stranded DNA under defined conditions (time, pH, temperature) and subsequent elution from the column allows selection of DNAzymes that undergo cleavage at the internal RNA bond in the presence of the metal ion of choice. The selected DNAzymes can be amplified via PCR and used to seed the following round of selection. The activity of the selected enzymes can be improved by gradually using more stringent conditions (such as shorter incubation times or lower temperatures) in each subsequent round of selection. The metal-binding affinity of the enzymes may also be improved by gradually decreasing the concentration of the metal ion. The selection continues until the generation at which improvement of activity stops. The DNAzymes can then be cloned and sequenced. Adapted from reference [102].

to design a colorimetric Pb^{2+} sensor. The primary and secondary structure of the “8-17” DNAzyme is presented in Fig. 4A. In the presence of Pb^{2+} , the substrate strand (17DS) can be cleaved by the enzyme strand (17E) at the scissile ribo-adenosine position (rA) (Fig. 4B). Through this work, the feasibility of using gold nanoparticles as colorimetric assay tools for DNA/RNAzymes has been validated. Comparisons are made for aggregates assembled by simple complementary DNA and by DNAzymes. As an example of the application of the colorimetric Pb^{2+} sensor, the detection of Pb^{2+} in leaded paint is also shown. The potential of using allosteric DNA/RNAzymes (aptazymes) to expand the range of analytes that the DNA/RNAzyme-nanoparticles-based sensor design strategy can apply is also presented at the end of the review.

GOLD NANOPARTICLES DO NOT INTERFERE WITH DNAZYME ACTIVITIES

One of the concerns about the design of colorimetric biosensors using DNAzyme-assembled gold nanoparticles is that nanoparticles might interfere with the activity of DNAzymes, for example, by absorbing DNAzymes or target analytes onto nanoparticle surfaces. To investigate whether the DNAzyme maintains the same activity in the presence of nanoparticles (functionalized with DNA), a biochemical assay was performed using a procedure described elsewhere [104,107,114]. The “8-17” DNAzyme cleaves its substrate in the presence of Pb^{2+} with the same efficiency, regardless of the presence or absence of gold nanoparticles (Fig. 2). This result suggests that the interaction between DNA-functionalized gold nanoparticles with other reagents in the reaction solution is minimal. This minimal interaction should also be related to the design of the sensor system (*vide infra*).

STRUCTURE SIMILARITY BETWEEN DNA- AND DNAZYME-ASSEMBLED NANOPARTICLE AGGREGATES

Nanoparticle aggregates assembled by complementary DNA strands reported by Mirkin and co-workers

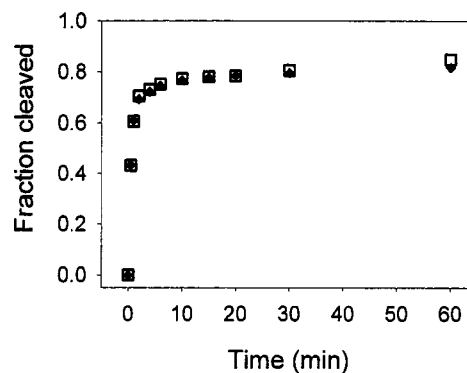


Fig. 2. The 17E DNAzyme activity assay in the presence (solid diamonds) and absence (open squares) of 12-mer DNA attached 13 nm diameter gold nanoparticles (DNA_{Au}). The reaction was carried out in 25 mM Tris-acetate buffer pH 7.2; 300 mM NaCl. $5 \mu\text{M}$ Pb^{2+} was added to initiate the cleavage reaction. The ^{32}P -labeled substrate (17DS) concentration was about 1 nM. The 17E concentration was $5 \mu\text{M}$. The DNA-linked gold nanoparticles (DNA_{Au}) were prepared according to procedures in [5] and their concentration was estimated to be 8 nM. The size of the gold nanoparticles was verified to be 13 nm by TEM (JEOL 2010). The cleaved and uncleaved substrates were separated by 20% polyacrylamide gel electrophoresis. The percentage of cleavage was quantified using a Fuji FLA-3000 PhosphorImager.

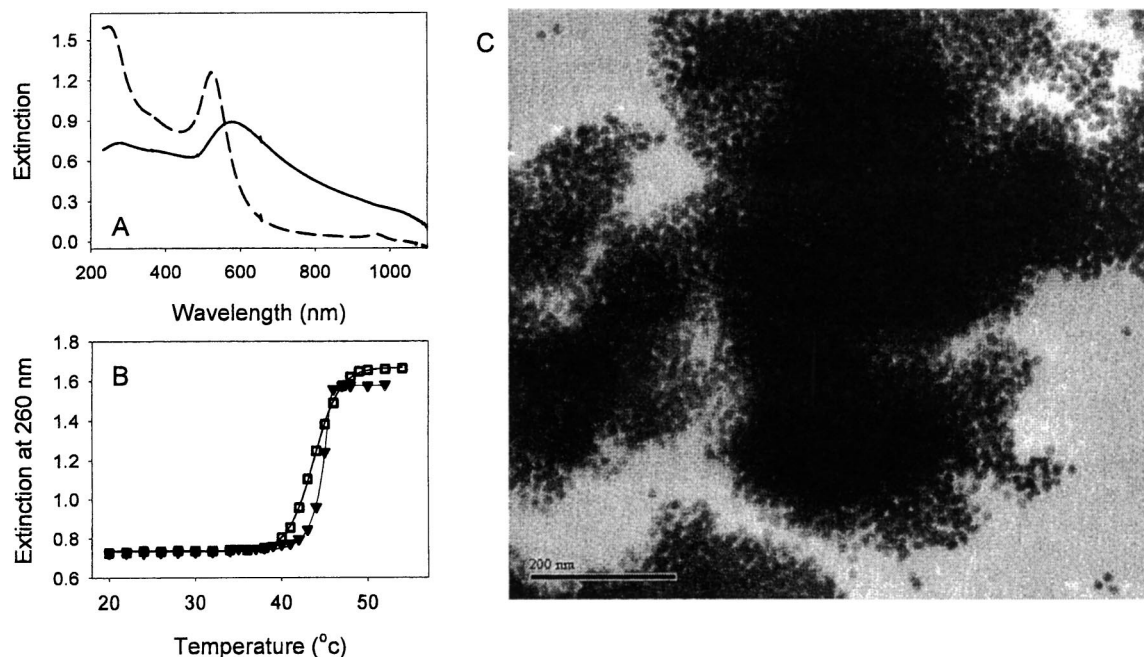


Fig. 3. (A). The UV-vis extinction spectrum of the DNAzyme-assembled 13 nm diameter gold nanoparticle aggregates (solid line) and the spectrum of separated nanoparticles after the melting of the aggregate (dashed line). (B). The melting curve of the nanoparticle aggregates that assembled by the DNAzyme (solid triangles), and by simple complementary strand DNA (sequence: 5'-CATCTCTTCCTATAGTGAGT-3') (empty squares). The melting curves were measured in 300 mM NaCl, 25 mM Tris-acetate buffer, pH 7.2. The melting temperatures were determined to be 46°C for the DNAzyme-assembled aggregates and 44°C for the DNA-assembled aggregates. (C). A TEM image of the DNAzyme-assembled 13 nm gold nanoparticle aggregates. The scale bar corresponds to 200 nm.

possess characteristic melting properties, which are distinguished by a very sharp melting transition and by a significant increase in the extinction at 260 nm compared to the melting of double-stranded DNA without nanoparticles [4,115,116]. Thus, the unique melting curve is an important property of the DNA-nanoparticle system. Therefore, measuring the melting curve of the DNAzyme-assembled nanoparticle aggregates should give information on whether the nanoparticles assembled by simple complementary DNA and by DNAzymes share similar structures. In Fig. 3A, the UV-vis extinction spectra of the DNAzyme-assembled nanoparticle aggregates (solid line) and separated nanoparticles after melting of the aggregates by heating (dashed line) is shown. As can be observed, after melting, the extinction at 260 nm and at 522 nm increases, while the extinction in the 700 nm region decreases. The increase in extinction at 260 nm is used to monitor the melting of nanoparticle aggregates. The melting curve of DNAzyme-assembled aggregates is shown in Fig. 3B (solid triangles). By replacing 17E with a DNA strand that is complementary to 17DS, nanoparticle aggregates can also be formed. In these aggregates, all DNA are in fully complementary state, similar to

the nanoparticle aggregates reported by Mirkin and co-workers [4,115,116]. The melting curve of these aggregates is also measured (Fig. 3B, open squares). The two melting curves share many similarities. The two aggregates have similar melting temperatures (see the figure legend). Both of the melting curves feature a sharp melting transition and a very large increase in the extinction at 260 nm. The similar melting properties suggest that the DNAzyme-assembled nanoparticle aggregates have a similar structure as DNA-assembled aggregates, even though a bulge is present in the DNAzyme (see Fig. 4A). The structure of the DNAzyme-assembled nanoparticle aggregates was also characterized by transmission electron microscopy (Fig. 3C); structures similar to DNA-assembled aggregates were observed [3]. Therefore, although DNAzymes have special secondary structures that are required for their catalytic activities, the aggregates assembled by DNAzymes have a similar structure to simple complementary DNA-assembled aggregates. This similarity allows us to employ the well-characterized properties of DNA-assembled nanoparticle aggregates for further design and optimization of DNAzyme-nanoparticle-based sensors.

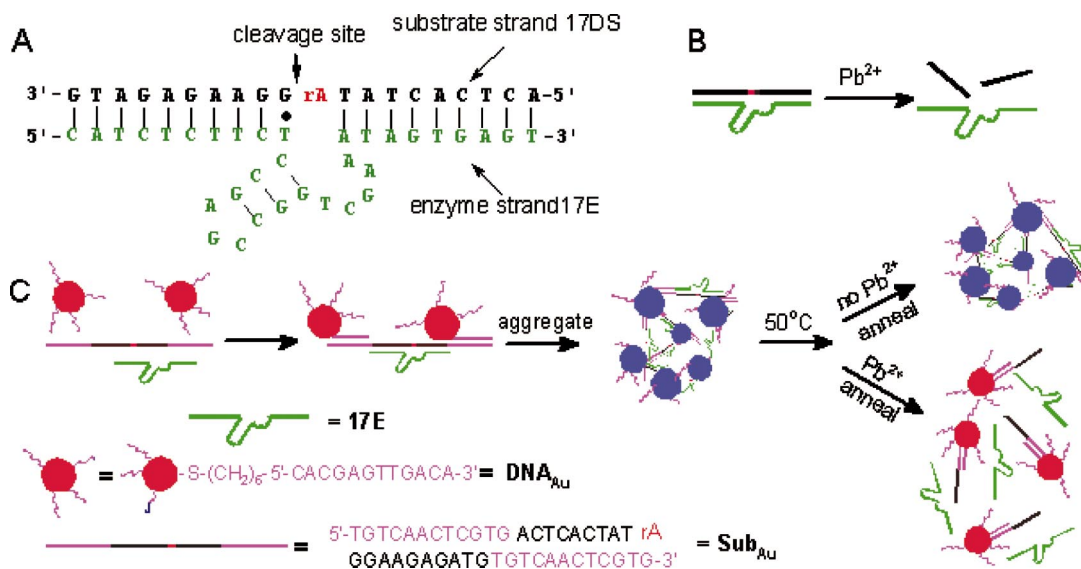


Fig. 4. (A) The secondary structure of the “8-17” DNAzyme system that consists of an enzyme strand (17E) and a substrate strand (17DS). The cleavage site is indicated by a black arrow. Except for a ribonucleoside adenosine at the cleavage site (rA), all other nucleosides are deoxyribonucleosides. (B) Cleavage of 17DS by 17E in the presence of Pb²⁺. (C) Schematics of the DNAzyme-directed assembly of gold nanoparticles and their application as biosensors for metal ions such as Pb²⁺. In this system, 17DS has been extended on both the 3' and 5' ends for 12 bases (the extended 17DS is named Sub_{Au}), which are complementary to the 12-mer DNA attached to the 13 nm gold nanoparticles (DNA_{Au}). See text for the description of the sensor design.

DESIGN OF THE COLORIMETRIC BIOSENSOR

The cleavage of the substrate strand in the presence of Pb²⁺ is the basis of the Pb²⁺ sensor design (Fig. 4B). The DNA sequence on gold nanoparticles can be designed in such a way that the uncleaved substrate can act as a linker to assemble gold nanoparticles, while the cleaved substrate cannot assemble nanoparticles. We chose to extend the substrate strand (17DS) at both ends for 12 bases and use the 12-base overhangs on each end to hybridize with DNA on nanoparticles. In this way, the enzyme binding region on the substrate strand is intact, and the binding of the substrate to nanoparticles should have little effect on the enzyme binding to the substrate. Therefore, the high sensitivity and selectivity of the DNAzyme for Pb²⁺ can be maintained.

In the initial design, the sensor contains three components, the enzyme strand (17E), the extended substrate strand (named Sub_{Au}), and DNA-functionalized gold nanoparticles (named DNA_{Au}) (Fig. 4C). To make the system as simple as possible, the two 12-base nanoparticle hybridizing regions on the substrate strand have identical sequences, so that nanoparticles are only functionalized with one kind of DNA [117]. The three components can anneal because of DNA base pairing interactions. Since there are over one hundred DNA molecules attached to each nanoparticle [118], the annealed product can cross-link to form large nanoparticle aggregates, which have a

blue color. The blue-colored aggregates have sizes ranging from several hundred nanometers to over one micrometer, based on TEM characterization. The relatively large size of nanoparticle aggregates makes them easy to isolate and purify by simple centrifugation. The purified aggregates can then be used as a colorimetric biosensor to detect Pb²⁺.

For the detection, nanoparticle aggregates are heated above the melting temperature of the aggregates (46°C) and allowed to cool slowly in a dry-bath to room temperature in a time course of ~2 hr. The aggregates contain gold nanoparticles, the substrate and the enzyme strand. After melting, the aggregates break into separated nanoparticles and the substrate and enzyme strands. In the process of cooling, the enzyme strand anneals to the substrate strand. The annealed product is either by cleaved in the presence of Pb²⁺, or acts as a linker to assemble gold nanoparticles. If nanoparticle aggregates can grow large enough, the substrate strand is protected in the aggregates from further cleavage. Because the rate of cleavage is dependent on the Pb²⁺ concentration, a higher Pb²⁺ concentration gives a faster cleavage rate. As a result, the substrate available to assemble nanoparticles decreases, resulting in a larger fraction of nanoparticles in the separated state and a red color. If no Pb²⁺ is present, the substrate is not cleaved and the nanoparticles can re-assemble and give blue colored aggregates. Thus, from the color developed by the sensor, the Pb²⁺ concentration can be quantified (Fig. 4C).

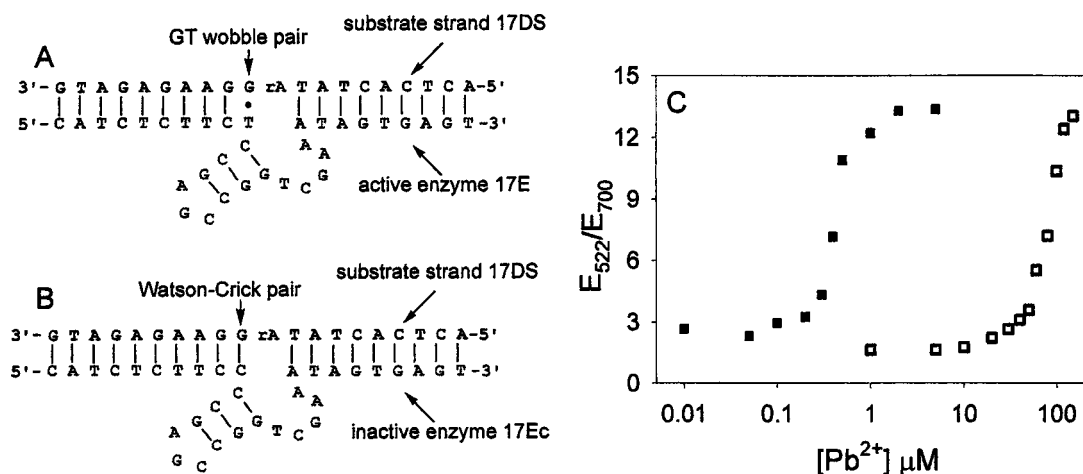


Fig. 5. (A). The structure of the active DNAzyme (17E). The G • T wobble pair that is crucial for the activity of the DNAzyme is highlighted by a black dot under the arrow. (B). The structure of the inactive DNAzyme (17Ec), in which the wobble pair is replaced by a Watson-Crick base pair. (C) Pb^{2+} detection level of the sensor. When the enzyme strand is the active 17E only, the Pb^{2+} detection range is from 0.1 μM to 4 μM (solid squares). When the ratio of 17E and 17Ec is 1:20, the Pb^{2+} detection range is from 10 μM to 200 μM (open squares).

A HIGHLY SENSITIVE AND SELECTIVE SENSOR WITH TUNABLE DETECTION RANGE

The color of the resulting sensor solution after the Pb^{2+} detection process described above can be conveniently monitored by UV-vis extinction spectroscopy. Upon aggregation, the extinction at 522 nm decreases, while the extinction at 700 nm increases (Fig. 3A). Thus, the ratio of extinction at 522 nm and 700 nm was used to characterize the degree of nanoparticle aggregation. A higher extinction ratio correlates with a lower degree of aggregation, or more nanoparticles in the separated states, and vice versa. The ratiometric method minimizes the differences between each experiment, such as the difference in nanoparticle concentration. As shown in Fig. 5C (solid squares), this un-optimized sensor can detect and quantify Pb^{2+} from 0.1 to 4 μM .

A unique feature of this DNAzyme-based sensor is that the detection range can be tuned over several orders of magnitude by using a mixture of active and inactive DNAzymes. The active DNAzyme contains a G • T wobble pair downstream of the substrate cleavage site (highlighted by a black dot in Fig. 5A). This wobble pair is essential for the activity of the DNAzyme [104,107,114]. If the wobble pair is replaced by a Watson-Crick base pair, e.g. by exchanging the T in the enzyme strand for a C base, the activity of the DNAzyme is abolished completely (Fig. 5B). However, the inactive DNAzyme has a similar structure to the active DNAzyme, and thus is also capable of assembling gold nanoparticles with similar optical properties. When a mixture of active and inac-

tive DNAzymes is used, a higher concentration of Pb^{2+} is needed to achieve the same degree of cleavage. Therefore, the detection range can be tuned to higher Pb^{2+} concentrations. For example, by using a ratio of 20:1 of inactive to active enzyme, the detection range is shifted to detect Pb^{2+} from 10 to 200 μM (Fig. 5C, open squares). The color of the sensor after detecting Pb^{2+} can be visualized by spotting the sensor onto a solid surface, such as an alumina TLC plate. Shown in Fig. 6B is the color developed on a TLC plate with different concentrations of Pb^{2+} . A blue to purple to red color progression can be observed. With other divalent metal ions, the color of the sensor remains blue (Fig. 6C), suggesting the high selectivity of the sensor.

APPLICATIONS: DETECTION OF LEAD IN LEADED PAINT

As described previously, one of the advantages of using DNA molecules as biosensor components is the high stability of DNA. DNA can withstand for rather harsh conditions and can still maintain binding or catalytic activities. We have already demonstrated that using the same DNAzyme labeled with fluorophore and quenchers, Pb^{2+} in Lake Michigan water could be detected [119]. By using the nanoparticle-based colorimetric biosensor, we have demonstrated that even Pb^{2+} in leaded paint can be quantitatively detected. The reason that we are interested in developing sensors to detect Pb^{2+} in paint is because ~24 million housing units in the United States

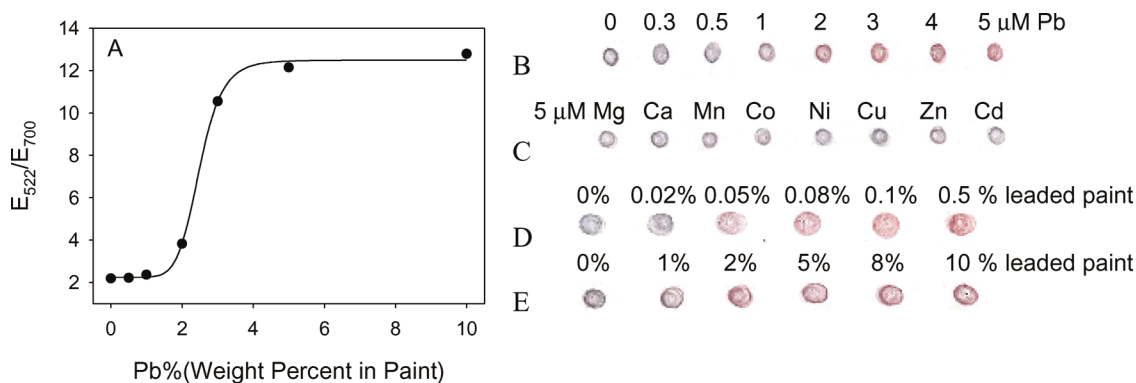


Fig. 6. (A). The quantification of Pb^{2+} in leaded paint using UV-vis spectroscopy. Typically, 0.1 g of leaded paint with different percentages of Pb^{2+} was soaked in 100 μL of 10% acetic acid solution. The soaking solution was diluted 150000 times for the detection. The detection procedures were the same as that for the detection of Pb^{2+} in water samples. The color of the sensor developed on an alumina TLC plate with different Pb^{2+} concentrations (B) and with 5 μM of 8 other divalent metal ions (C). The reactions in both (B) and (C) are carried out in 25 mM Tris-acetate buffer, pH 7.2, containing 300 mM NaCl. Colorimetric detection and quantification of lead in leaded paint. The color developed on a TLC plate by the sensor after reacting with 360- (C) and 15,000-fold (D) dilution of the soaking solution for the leaded paint. The pictures were acquired with an EPSON Perfection 1200S scanner.

have deteriorated leaded paint and elevated levels of lead-contaminated house dust, according to the U.S. Centers for Disease Control (CDC) [120]. Current methods for Pb^{2+} detection in leaded paint are prone to false positive or false negative results [121,122]. Given the high stability of DNA, the high sensitivity and selectivity of the DNAzyme-based Pb^{2+} sensor, and its capability of providing simple colorimetric detection, it is very attractive to apply this sensor for on-site, real time detection of Pb^{2+} in leaded paint. We made leaded paint samples with different percentages of Pb^{2+} added. After drying the leaded paint, Pb^{2+} was extracted by soaking with acetic acid solution. Because the amount of Pb^{2+} in leaded paint can be as high as 20%, dilution is needed for quantitative detection. Shown in Fig. 6A is the quantification of Pb^{2+} in leaded paint using UV-vis spectroscopy. A similar curve as in the detection of Pb^{2+} added to Millipore water was observed, indicating the method can not only be used to detect but also can quantify lead in paint. Similarly, the resulting sensor solution can be spotted onto a TLC plate for visualization. Shown in Fig. 6D and 6E are the colors developed by the sensor for two different concentration ranges of Pb^{2+} in leaded paint. In each case, a blue to red color transition with increasing Pb^{2+} percentage was observed.

PERSPECTIVES

The design of a colorimetric Pb^{2+} sensor using DNAzyme-assembled gold nanoparticles has been

demonstrated, which shows potential practical applications, such as the detection and quantification of Pb^{2+} in leaded paint [117]. Given the vast amount of analytes that need to be detected and quantified with high accuracy and certainty for civilian, industrial, environmental, and military applications [123], it would be desirable for this methodology to be generalized to the detection of all analytes that can be recognized by DNA/RNA aptamers listed in Table I. Comparing the analytes that DNAzymes can recognize in Table III to those that aptamers can recognize in Table I, it can be seen that most DNAzymes use only metal ions as cofactors, while the range of analytes that aptamers can recognize is much wider.

Some recent development in the catalytic DNA/RNA field has resulted in a new class of DNA/RNAzymes, which combine an aptamer motif with a DNA/RNAzyme catalytic core and are known as allosteric DNA/RNAzymes or aptazymes [18,124–126]. Upon analytes binding to the aptamer motif, the tertiary structure of an aptazyme is activated and can cleave the corresponding substrate. Aptazymes can be obtained through either *in vitro* selection [19,127,128] or through rational design [124,125]. One example of an aptazyme that contains an ATP or adenosine aptamer motif is shown in Fig. 7. This is an example of the rationally designed aptazymes that can recognize ATP or adenosine [125,129]. Similarly, the substrate strand of the aptazyme can be extended on both ends to hybridize to DNA on nanoparticles for detection purposes. The invention of aptazymes should expand the scope of the DNAzyme-nanoparticle methodology to the detection of a very wide range of important analytes [130].

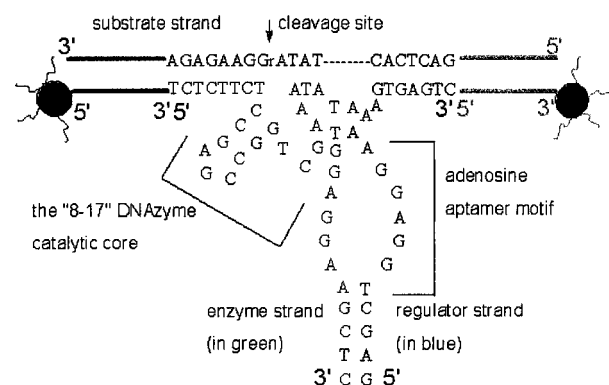


Fig. 7. Expanding the range of analytes that DNAzyme-based sensors can detect by using allosteric DNAzymes (aptazymes). As an example, the primary and the proposed secondary structure of an ATP or adenosine aptazyme built on the “8–17” DNAzyme platform is shown [44]. This aptazyme is composed of a substrate strand, an enzyme strand and a regulator strand. The 3′-end of the enzyme strand and the 5′-end of the regulator strand form an ATP or adenosine aptamer motif. Upon binding to an ATP or adenosine molecule, the aptazyme is activated and can cleave its substrate. The substrate strand is extended on both ends so that it can assemble nanoparticles for sensor applications [130].

ACKNOWLEDGMENTS

This material is based upon work supported by the U.S. Department of Energy (NABIR program, DEFG02-01-ER63179) and by Nanoscale Science and Engineering Initiative of the National Science Foundation (DMR-0117792).

REFERENCES

- H. B. Weiser (1933). *Inorganic Colloid Chemistry, Vol. 1*, Wiley, New York.
- D. A. Handley (1989). In M. A. Hayat (Ed.), *Colloidal Gold Principles, Methods, and Applications*, Academic Press, San Diego, CA, pp. 1–12.
- C. A. Mirkin, R. L. Letsinger, R. C. Mucic, and J. J. Storhoff (1996). A DNA-based method for rationally assembling nanoparticles into macroscopic materials. *Nature* **382**(6592), 607–609.
- R. Elghanian, J. J. Storhoff, R. C. Mucic, R. L. Letsinger, and C. A. Mirkin (1997). Selective colorimetric detection of polynucleotides based on the distance-dependent optical properties of gold nanoparticles. *Science* **277**(5329), 1078–1080.
- J. J. Storhoff, R. Elghanian, R. C. Mucic, C. A. Mirkin, and R. L. Letsinger (1998). One-pot colorimetric differentiation of polynucleotides with single base imperfections using gold nanoparticle probes. *J. Am. Chem. Soc.* **120**(9), 1959–1964.
- T. A. Taton, C. A. Mirkin, and R. L. Letsinger (2000). Scanometric DNA array detection with nanoparticle probes. *Science* **289**(5485), 1757–1760.
- Y. Cao, R. Jin, and C. A. Mirkin (2001). DNA-modified core-shell Ag/Au nanoparticles. *J. Am. Chem. Soc.* **123**(32), 7961–7962.
- G. P. Mitchell, C. A. Mirkin, and R. L. Letsinger (1999). Programmed assembly of DNA functionalized quantum dots. *J. Am. Chem. Soc.* **121**(35), 8122–8123.

- R. Chakrabarti and A. M. Klivanov (2003). Nanocrystals modified with peptide nucleic acids (PNAs) for selective self-assembly and DNA detection. *J. Am. Chem. Soc.* **125**(41), 12531–12540.
- K. Sato, K. Hosokawa, and M. Maeda (2003). Rapid aggregation of gold nanoparticles induced by non-cross-linking DNA hybridization. *J. Am. Chem. Soc.* **125**(27), 8102–8103.
- L. Gold, B. Polisky, O. Uhlenbeck, and M. Yarus (1995). Diversity of oligonucleotide functions. *Annu. Rev. Biochem.* **64**, 763–797.
- S. E. Osborne and A. D. Ellington (1997). Nucleic acid selection and the challenge of combinatorial chemistry. *Chem. Rev.* **97**(2), 349–370.
- R. R. Breaker (1997). In vitro selection of catalytic polynucleotides. *Chem. Rev.* **97**(2), 371–390.
- D. S. Wilson and J. W. Szostak (1999). In vitro selection of functional nucleic acids. *Annu. Rev. Biochem.* **68**, 611–647.
- G. F. Joyce and L. E. Orgel (1999). In R. F. Gesteland, T. R. Cech, and J. F. Atkins (Ed.), *RNA World*, 2nd ed., Cold Spring Harbor Laboratory Press, Cold Spring Harbor, New York, pp. 49–77.
- S. D. Jayasena (1999). Aptamers: An emerging class of molecules that rival antibodies in diagnostics. *Clin. Chem.* **45**(9), 1628–1650.
- E. N. Brody and L. Gold (2000). Aptamers as therapeutic and diagnostic agents. *Rev. Mol. Biotech.* **74**(1), 5–13.
- J. Hesselberth, M. P. Robertson, S. Jhaveri, and A. D. Ellington (2000). In vitro selection of nucleic acids for diagnostic applications. *Rev. Mol. Biotechnol.* **74**(1), 15–25.
- G. A. Soukup and R. R. Breaker (2000). Allosteric nucleic acid catalysts. *Curr. Opin. Struct. Biol.* **10**(3), 318–325.
- R. R. Breaker (2002). Engineered allosteric ribozymes as biosensor components. *Curr. Opin. Biotechnol.* **13**(1), 31–39.
- H. Ueyama, M. Takagi, and S. Takenaka (2002). A novel potassium sensing in aqueous media with a synthetic oligonucleotide derivative. Fluorescence resonance energy transfer associated with guanine quartet-potassium ion complex formation. *J. Am. Chem. Soc.* **124**(48), 14286–14287.
- J. Ciesiolka and M. Yarus (1996). Small RNA-divalent domains. *RNA* **2**(8), 785–793.
- H. P. Hofmann, S. Limmer, V. Hornung, and M. Sprinzl (1997). Ni²⁺-binding RNA motifs with an asymmetric purine-rich internal loop and a G-A base pair. *RNA* **3**(11), 1289–1300.
- A. D. Ellington and J. W. Szostak (1992). Selection in vitro of single-stranded DNA molecules that fold into specific ligand-binding structures. *Nature* **355**(6363), 850–852.
- A. D. Ellington and J. W. Szostak (1990). In vitro selection of RNA molecules that bind specific ligands. *Nature* **346**(6287), 818–822.
- C. Wilson and J. W. Szostak (1998). Isolation of a fluorophore-specific DNA aptamer with weak redox activity. *Chem. Biol.* **5**(11), 609–617.
- D. Grate and C. Wilson (1999). Laser-mediated, site-specific inactivation of RNA transcripts. *Proc. Natl. Acad. Sci. U.S.A.* **96**(11), 6131–6136.
- C. Wilson, J. Nix, and J. Szostak (1998). Functional requirements for specific ligand recognition by a biotin-binding RNA pseudoknot. *Biochemistry* **37**(41), 14410–14419.
- M. N. Stojanovic, P. de Prada, and D. W. Landry (2000). Fluorescent sensors based on aptamer self-assembly. *J. Am. Chem. Soc.* **122**(46), 11547–11548.
- G. R. Zimmermann, C. L. Wick, T. P. Shields, R. D. Jenison, and A. Pardi (2000). Molecular interactions and metal binding in the theophylline-binding core of an RNA aptamer. *RNA* **6**(5), 659–667.
- M. Meli, J. Vergne, J.-L. Decout, and M.-C. Maurel (2002). Adenine-aptamer complexes. A bipartite RNA site that binds the adenine nucleic base. *J. Biol. Chem.* **277**(3), 2104–2111.
- C. Mannironi, A. Di Nardo, P. Fruscoloni, and G. P. Tocchini-Valentini (1997). In vitro selection of dopamine RNA ligands. *Biochemistry* **36**(32), 9726–9734.
- I. Majerfeld and M. Yarus (1994). An RNA pocket for an aliphatic hydrophobe. *Nat. Struct. Biol.* **1**(5), 287–292.

34. M. Famulok and J. W. Szostak (1992). Stereospecific recognition of tryptophan agarose by in vitro selected RNA. *J. Am. Chem. Soc.* **114**(10), 3990–3991.
35. K. Harada and A. D. Frankel (1995). Identification of two novel arginine binding DNAs. *EMBO J.* **14**(23), 5798–5811.
36. G. J. Connell, M. Illangsekare, and M. Yarus (1993). Three small ribooligonucleotides with specific arginine sites. *Biochemistry* **32**(21), 5497–5502.
37. J. Tao and A. D. Frankel (1996). Arginine-binding RNAs resembling TAR identified by in vitro selection. *Biochemistry* **35**(7), 2229–2238.
38. M. Famulok (1994). Molecular recognition of amino acids by RNA-aptamers: An L-citrulline binding RNA motif and its evolution into an L-arginine binder. *J. Am. Chem. Soc.* **116**(5), 1698–1706.
39. G. J. Connell and M. Yarus (1994). RNAs with dual specificity and dual RNAs with similar specificity. *Science* **264**(5162), 1137–1141.
40. N. K. Vaish, R. Larralde, A. W. Fraley, J. W. Szostak, and L. W. McLaughlin (2003). A novel, modification-dependent ATP-binding aptamer selected from an RNA library incorporating a cationic functionality. *Biochemistry* **42**(29), 8842–8851.
41. M. Sassanfar and J. W. Szostak (1993). An RNA motif that binds ATP. *Nature* **364**(6437), 550–553.
42. J. H. Davis and J. W. Szostak (2002). Isolation of high-affinity GTP aptamers from partially structured RNA libraries. *Proc. Natl. Acad. Sci. U.S.A.* **99**(18), 11616–11621.
43. M. Koizumi and R. R. Breaker (2000). Molecular recognition of cAMP by an RNA aptamer. *Biochemistry* **39**(30), 8983–8992.
44. S. M. Rink, J.-C. Shen, and L. A. Loeb (1998). Creation of RNA molecules that recognize the oxidative lesion 7,8-dihydro-8-hydroxy-2'-deoxyguanosine (8-oxodG) in DNA. *Proc. Natl. Acad. Sci. U.S.A.* **95**(20), 11619–11624.
45. C. Boiziau, E. Dausse, L. Yurchenko, and J.-J. Toulme (1999). DNA aptamers selected against the HIV-1 trans-activation-responsive RNA element form RNA-DNA kissing complexes. *J. Biol. Chem.* **274**(18), 12730–12737.
46. C. T. Lauhon and J. W. Szostak (1995). RNA aptamers that bind flavin and nicotinamide redox cofactors. *J. Am. Chem. Soc.* **117**(4), 1246–1257.
47. P. Burgstaller and M. Famulok (1994). Isolation of RNA aptamers for biological cofactors by in vitro selection *Angew. Chem.* **106**(10), 1163–1166 (see also *Angew. Chem., Int. Ed. Engl.* **1133**(1110), 1084–1167(1994)).
48. D. J. F. Chinnapan and D. Sen (2002). Hemin-stimulated docking of cytochrome *c* to a Hemin-DNA aptamer complex. *Biochemistry* **41**(16), 5202–5212.
49. J. R. Lorsch and J. W. Szostak (1994). In vitro selection of RNA aptamers specific for cyanocobalamin. *Biochemistry* **33**(4), 973–982.
50. M. Roychowdhury-Saha, S. M. Lato, E. D. Shank, and D. H. Burke (2002). Flavin recognition by an RNA aptamer targeted toward FAD. *Biochemistry* **41**(8), 2492–2499.
51. D. Burke and D. Hoffman (1998). A novel acidophilic RNA motif that recognizes coenzyme A. *Biochemistry* **37**(13), 4653–4663.
52. Y. Wang, J. Killian, K. Hamasaki, and R. R. Rando (1996). RNA molecules that specifically and stoichiometrically bind aminoglycoside antibiotics with high affinities. *Biochemistry* **35**(38), 12338–12346.
53. M. G. Wallis, U. von Ahsen, R. Schroeder, and M. Famulok (1995). A novel RNA motif for neomycin recognition. *Chem. Biol.* **2**(8), 543–552.
54. Q. Yang, I. J. Goldstein, H.-Y. Mei, and D. R. Engelke (1998). DNA ligands that bind tightly and selectively to cellobiose. *Proc. Natl. Acad. Sci. U.S.A.* **95**(10), 5462–5467.
55. C. Srisawat, I. J. Goldstein, and D. R. Engelke (2001). Sephadex-binding RNA ligands: Rapid affinity purification of RNA from complex RNA mixtures. *Nucleic Acids Res.* **29**(2), E41–E45.
56. S. T. Wallace and R. Schroeder (1998). In vitro selection and characterization of streptomycin-binding RNAs: Recognition discrimination between antibiotics. *RNA* **4**(1), 112–123.
57. M. G. Wallis, B. Streicher, H. Wank, U. von Ahsen, E. Clodi, S. T. Wallace, M. Famulok, and R. Schroeder (1997). In vitro selection of a viomycin-binding RNA pseudoknot. *Chem. Biol.* **4**(5), 357–366.
58. C. Berens, A. Thain, and R. Schroeder (2001). A tetracycline-binding RNA aptamer. *Bioorg. Med. Chem.* **9**(10), 2549–2556.
59. L. Giver, D. Bartel, M. Zapp, A. Pawul, M. Green, and A. D. Ellington (1993). Selective optimization of the Rev-binding element of HIV-1. *Nucleic Acids Res.* **21**(23), 5509–5516.
60. K. P. Williams, X.-H. Liu, T. N. M. Schumacher, H. Y. Lin, D. A. Ausiello, P. S. Kim, and D. P. Bartel (1997). Bioactive and nuclease-resistant L-DNA ligand of vasopressin. *Proc. Natl. Acad. Sci. U.S.A.* **94**(21), 11285–11290.
61. D. Nieuwlandt, M. Wecker, and L. Gold (1995). In vitro selection of RNA ligands to substance P. *Biochemistry* **34**(16), 5651–5659.
62. L. C. Bock, L. C. Griffin, J. A. Latham, E. H. Vermaas, and J. J. Toole (1992). Selection of single-stranded DNA molecules that bind and inhibit human thrombin. *Nature* **355**(6360), 564–566.
63. C. Tuerk, S. MacDougal, and L. Gold (1992). RNA pseudoknots that inhibit human immunodeficiency virus type 1 reverse transcriptase. *Proc. Natl. Acad. Sci. U.S.A.* **89**(15), 6988–6992.
64. M. Vuyisich and P. A. Beal (2002). Controlling protein activity with ligand-regulated RNA aptamers. *Chem. Biol.* **9**(8), 907–913.
65. F. Pileur, M.-L. Andreola, E. Dausse, J. Michel, S. Moreau, H. Yamada, S. A. Gaidamakov, R. J. Crouch, J.-J. Toulme, and C. Cazenave (2003). Selective inhibitory DNA aptamers of the human RNase H1. *Nucleic Acids Res.* **31**(19), 5776–5788.
66. N. C. Pagratis, C. Bell, Y.-F. Chang, S. Jennings, T. Fitzwater, D. Jellinek, and C. Dang (1997). Potent 2'-amino-, and 2'-fluoro-2'-deoxyribonucleotide RNA inhibitors of keratinocyte growth factor. *Nature Biotech.* **15**(1), 68–73.
67. D. Jellinek, L. S. Green, C. Bell, C. K. Lynott, N. Gill, C. Vargeese, G. Kirschheuter, D. P. C. McGee, P. Abesinghe, *et al.* (1995). Potent 2'-amino-2'-deoxypyrimidine RNA inhibitors of basic fibroblast growth factor. *Biochemistry* **34**(36), 11363–11372.
68. J. Ruckman, L. S. Green, J. Beeson, S. Waugh, W. L. Gillette, D. D. Henninger, L. Claesson-Welsh, and N. Janjic (1998). 2'-fluoropyrimidine RNA-based aptamers to the 165-amino acid form of vascular endothelial growth factor (VEGF165). Inhibition of receptor binding and VEGF-induced vascular permeability through interactions requiring the exon 7-encoded domain. *J. Biol. Chem.* **273**(32), 20556–20567.
69. L. L. Lebruska and L. J. Maher III (1999). Selection and characterization of an RNA decoy for transcription factor NF- κ B. *Biochemistry* **38**(10), 3168–3174.
70. T. W. Wiegand, P. B. Williams, S. C. Dreskin, M. H. Jouvin, J. P. Kinet, and D. Tasset (1996). High-affinity oligonucleotide ligands to human IgE inhibit binding to Fc epsilon receptor I. *J. Immun.* **157**(1), 221–230.
71. I. A. Nazarenko and O. C. Uhlenbeck (1995). Defining a smaller RNA substrate for elongation factor Tu. *Biochemistry* **34**(8), 2545–2552.
72. K. A. Davis, Y. Lin, B. Abrams, and S. D. Jayasena (1998). Staining of cell surface human CD4 with 2'-F-pyrimidine-containing RNA aptamers for flow cytometry. *Nucleic Acids Res.* **26**(17), 3915–3924.
73. S. Jeong, T.-Y. Eom, S.-J. Kim, S.-W. Lee, and J. Yu (2001). In vitro selection of the RNA aptamer against the Sialyl Lewis X and its inhibition of the cell adhesion. *Biochem. Biophys. Res. Commun.* **281**(1), 237–243.
74. M. Blank, T. Weinschenk, M. Priemer, and H. Schluesener (2001). Systematic evolution of a DNA aptamer binding to rat brain tumor microvessels. Selective targeting of endothelial regulatory protein p16. *J. Biol. Chem.* **276**(19), 16464–16468.
75. W. Pan, R. C. Craven, Q. Qiu, C. B. Wilson, J. W. Wills, S. Golovine, and J.-F. Wang (1995). Isolation of virus-neutralizing RNAs from a large pool of random sequences. *Proc. Natl. Acad. Sci. U.S.A.* **92**(25), 11509–11513.

76. J. G. Bruno and J. L. Kiel (1999). In vitro selection of DNA aptamers to anthrax spores with electrochemiluminescence detection. *Biosens. Bioelectr.* **14**(5), 457–464.
77. J. Tsang and G. F. Joyce (1996). In vitro evolution of randomized ribozymes. *Methods Enzymol.* **267**(Combinatorial Chemistry), 410–426.
78. R. R. Breaker (1997). DNA enzymes. *Nat. Biotechnol.* **15**(5), 427–431.
79. R. R. Breaker (1997). DNA aptamers and DNA enzymes. *Curr. Opin. Chem. Biol.* **1**(1), 26–31.
80. D. Sen and C. R. Geyer (1998). DNA enzymes. *Curr. Opin. Chem. Biol.* **2**(6), 680–687.
81. M. Kurz and R. R. Breaker (1999). In vitro selection of nucleic acid enzymes. *Current Topics in Microbiology and Immunology* **243**(Combinatorial Chemistry in Biology), 137–158.
82. T. R. Cech (1987). The chemistry of self-splicing RNA and RNA enzymes. *Science* **236**(4808), 1532–1539.
83. T. R. Cech (2000). Perspectives. Structural biology: The ribosome is a ribozyme. *Science* **289**(5481), 878–879.
84. N. K. Vaish, P. A. Heaton, O. Fedorova, and F. Eckstein (1998). In vitro selection of a purine nucleotide-specific hammerhead-like ribozyme. *Proc. Natl. Acad. Sci. U.S.A.* **95**(5), 2158–2162.
85. E. H. Eklund, J. W. Szostak, and D. P. Bartel (1995). Structurally complex and highly active RNA ligases derived from random RNA sequences. *Science* **269**(5222), 364–370.
86. J. R. Lorsch and J. W. Szostak (1994). In vitro evolution of new ribozymes with polynucleotide kinase activity. *Nature* **371**(6492), 31–36.
87. E. H. Eklund and D. P. Bartel (1996). RNA-catalyzed RNA polymerization using nucleoside triphosphates. *Nature* **382**(6589), 373–376.
88. M. Illangasekare and M. Yarus (1997). Small-molecule-substrate interactions with a self-aminoacylating ribozyme. *J. Mol. Biol.* **268**(3), 631–639.
89. J. A. Piccirilli, T. S. McConnell, A. J. Zaug, H. F. Noller, and T. R. Cech (1992). Aminoacyl esterase activity of the Tetrahymena ribozyme. *Science* **256**(5062), 1420–1424.
90. P. A. Lohse and J. W. Szostak (1996). Ribozyme-catalyzed amino acid transfer reactions. *Nature* **381**(6581), 442–444.
91. C. Wilson and J. W. Szostak (1995). In vitro evolution of a self-alkylating ribozyme. *Nature* **374**(6525), 777–782.
92. M. Wecker, D. Smith, and L. Gold (1996). In vitro selection of a novel catalytic RNA: Characterization of a sulfur alkylation reaction and interaction with a small peptide. *RNA* **2**(10), 982–994.
93. X. Dai, A. De Mesmaeker, and G. F. Joyce (1995). Cleavage of an amide bond by a ribozyme. *Science* **267**(5195), 237–240.
94. T. W. Wiegand, R. C. Janssen, and B. E. Eaton (1997). Selection of RNA amide synthases. *Chem. Biol.* **4**(9), 675–683.
95. B. Zhang and T. R. Cech (1997). Peptide bond formation by in vitro selected ribozymes. *Nature* **390**(6655), 96–100.
96. T. M. Tarasow, S. L. Tarasow, C. Tu, E. Kellogg, and B. E. Eaton (1999). Characteristics of an RNA diels-alderase active site. *J. Am. Chem. Soc.* **121**(15), 3614–3617.
97. J. R. Prudent, T. Uno, and P. G. Schultz (1994). Expanding the scope of RNA catalysis. *Science* **264**(5167), 1924–1927.
98. M. M. Conn, J. R. Prudent, and P. G. Schultz (1996). Porphyrin metalation catalyzed by a small RNA molecule. *J. Am. Chem. Soc.* **118**(29), 7012–7013.
99. R. R. Breaker and G. F. Joyce (1994). A DNA enzyme that cleaves RNA. *Chem. Biol.* **1**(4), 223–229.
100. R. R. Breaker (2000). Making catalytic DNAs. *Science* **290**(5499), 2095–2096.
101. Y. Lu (2002). New transition metal-dependent DNAzymes as efficient endonucleases and as selective metal biosensors. *Chem. Eur. J.* **8**:4588–4596.
102. R. R. Breaker and G. F. Joyce (1995). A DNA enzyme with Mg²⁺-dependent RNA phosphoesterase activity. *Chem. Biol.* **2**(10), 655–660.
103. D. Faulhammer and M. Famulok (1997). Characterization and divalent metal-ion dependence of in vitro selected deoxyribozymes which cleave DNA/RNA chimeric oligonucleotides. *J. Mol. Biol.* **269**(2), 188–202.
104. S. W. Santoro and G. F. Joyce (1997). A general purpose RNA-cleaving DNA enzyme. *Proc. Natl. Acad. Sci. U. S. A.* **94**(9), 4262–4266.
105. C. R. Geyer and D. Sen (1997). Evidence for the metal-cofactor independence of an RNA phosphodiester-cleaving DNA enzyme. *Chem. Biol.* **4**(8), 579–593.
106. A. Roth and R. R. Breaker (1998). An amino acid as a cofactor for a catalytic polynucleotide. *Proc. Natl. Acad. Sci. U.S.A.* **95**(11), 6027–6031.
107. J. Li, W. Zheng, A. H. Kwon, and Y. Lu (2000). In vitro selection and characterization of a highly efficient Zn(II)-dependent RNA-cleaving deoxyribozyme. *Nucleic Acids Res.* **28**(2), 481–488.
108. N. Carmi, L. A. Shultz, and R. R. Breaker (1996). In vitro selection of self-cleaving DNAs. *Chem. Biol.* **3**(12), 1039–1046.
109. B. Cuenoud and J. W. Szostak (1995). A DNA metalloenzyme with DNA ligase activity. *Nature* **375**(6532), 611–614.
110. Y. Wang and S. K. Silverman (2003). Deoxyribozymes that synthesize branched and lariat RNA. *J. Am. Chem. Soc.* **125**(23), 6880–6881.
111. Y. Li and R. R. Breaker (1999). Phosphorylating DNA with DNA. *Proc. Natl. Acad. Sci. U.S.A.* **96**(6), 2746–2751.
112. Y. Li, Y. Liu, and R. R. Breaker (2000). Capping DNA with DNA. *Biochemistry* **39**(11), 3106–3114.
113. Y. Li and D. Sen (1996). A catalytic DNA for porphyrin metallation. *Nat. Struct. Biol.* **3**(9), 743–747.
114. D. Faulhammer and M. Famulok (1996). The Ca²⁺ ion as a cofactor for a novel RNA-cleaving deoxyribozyme. *Angew. Chem., Int. Ed. Engl.* **35**(23/24), 2837–2841.
115. J. J. Storhoff, A. A. Lazarides, R. C. Mucic, C. A. Mirkin, R. L. Letsinger, and G. C. Schatz (2000). What controls the optical properties of DNA-linked gold nanoparticle assemblies? *J. Am. Chem. Soc.* **122**(19), 4640–4650.
116. R. Jin, G. Wu, Z. Li, C. A. Mirkin, and G. C. Schatz (2003). What controls the melting properties of DNA-linked gold nanoparticle assemblies? *J. Am. Chem. Soc.* **125**(6), 1643–1654.
117. J. Liu and Y. Lu (2003). A colorimetric lead biosensor using DNAzyme-directed assembly of gold nanoparticles. *J. Am. Chem. Soc.* **125**(22), 6642–6643.
118. L. M. Demers, C. A. Mirkin, R. C. Mucic, R. A. Reynolds III, R. L. Letsinger, R. Elghanian, and G. Viswanadham (2000). A fluorescence-based method for determining the surface coverage and hybridization efficiency of thiol-capped oligonucleotides bound to gold thin films and nanoparticles. *Anal. Chem.* **72**(22), 5535–5541.
119. J. Liu and Y. Lu (2003). Improving fluorescent DNAzyme biosensors by combining inter- and intramolecular quenchers. *Anal. Chem.* **75**(23), 6666–6672.
120. U. S. Department of Housing and Urban Development (2001). Unpublished data, 2001.
121. K. K. Luk, L. L. Hodson, J. A. O'Rourke, D. S. Smith, and W. F. Gutknecht (1993). *Investigation of Test Kits for Detection of Lead in Paint, Dust, and Soil*, EPA 600/R-93/085, U.S. Environmental Protection Agency, Research Triangle Park, NC.
122. W. J. Rossiter Jr., M. G. Vangel, M. E. McKnight, and G. Dewalt (2000, March). *Spot Test Kits for Detecting Lead in Household Paint: A Laboratory Evaluation*, NISTIR 6398, National Institute of Standards and Technology, Gaithersburg, MD.
123. A. W. Czarnik (1995). Desperately seeking sensors. *Chem. Biol.* **2**(7), 423–428.
124. J. Tang and R. R. Breaker (1997). Rational design of allosteric ribozymes. *Chem. Biol.* **4**(6), 453–459.
125. D. Y. Wang, B. H. Y. Lai, and D. Sen (2002). A general strategy for effector-mediated control of RNA-cleaving ribozymes and DNA enzymes. *J. Mol. Biol.* **318**(1), 33–43.

126. M. Levy and A. D. Ellington (2002). ATP-dependent allosteric DNA enzymes. *Chem. Biol.* **9**(4), 417–426.
127. G. A. Soukup, G. A. M. Emilsson, and R. R. Breaker (2000). Altering molecular recognition of RNA aptamers by allosteric selection. *J. Mol. Biol.* **298**(4), 623–632.
128. G. A. Soukup, E. C. DeRose, M. Koizumi, and R. R. Breaker (2001). Generating new ligand-binding RNAs by affinity maturation and disintegration of allosteric ribozymes. *RNA* **7**(4), 524–536.
129. D. E. Huizenga and J. W. Szostak (1995). A DNA aptamer that binds adenosine and ATP. *Biochemistry* **34**(2), 656–665.
130. J. Liu and Y. Lu (2004). Adenosine dependent assembly of aptazyme-functionalized gold nanoparticles and their application as a colorimetric biosensor. *Anal. Chem.* **76**(6), 1627–1632.